Applications

Ajay Krishna, Ismael Jaramillo-Cajica*, Sabine Auer and Johannes Schiffer

A power-hardware-in-the-loop testbed for intelligent operation and control of low-inertia power systems

Ein PHIL-Prüfstand für den intelligenten Betrieb und die Regelung von Energiesystemen mit reduzierter Schwungmasse

https://doi.org/10.1515/auto-2022-0025
Received February 18, 2022; accepted October 17, 2022

Abstract: Low-inertia power systems, i.e., power-electronics-dominated power systems, possess significantly different dynamics to conventional power systems, both on a component and a system-wide level. A direct implication of these substantial changes is that a pure simulation-based assessment of novel control and operational schemes for such systems is insufficient. Instead, flexible and easily reconfigurable experimental testing facilities are required. A prominent concept to enable such capabilities is power-hardware-in-the-loop (PHiL) testing. We present a PHiL testbed facility (230/400 VAC, 750 VDC, 100 kW) specifically designed for experimentally testing and validating control and operational schemes for low-inertia power systems. The main features of the testbed are its flexibility to rapidly implement and test advanced control algorithms, ranging from low-level controls of individual components to distributed and system-wide controls, its ability to be configured with different network topologies, and the efficient emulation of commonly observed parameter uncertainties as well as disturbances. The detailed description of the PHiL testbed is complemented by a performance demonstration via a case study.

Keywords: distributed control applications; low-inertia power systems; power-hardware-in-the-loop test; smart grids.

Zusammenfassung: Elektrische Energiesysteme mit geringer Trägheit, d. h. Energiesysteme mit hohem Anteil leistungselektronischer Komponenten, weisen sowohl auf der Ebene einzelner Komponenten als auch auf der Ebene des Gesamtsystems eine deutlich andere Dynamik auf als konventionelle Energiesysteme. Eine unmittelbare Folge dieser wesentlichen Veränderungen ist, dass eine rein simulationsbasierte Bewertung neuartiger Regelungs-und Betriebsverfahren für solche Systeme unzureichend ist. Stattdessen werden flexible und leicht rekonfigurierbare experimentelle Testeinrichtungen benötigt. Ein bekanntes Konzept zur Ermöglichung solcher Fähigkeiten ist Power-Hardware-in-the-Loop (PHiL). Wir stellen ein PHiL-Prüffeld (230/400 VAC, 750 VDC, 100 kW) vor, das speziell für die experimentelle Prüfung und Validierung von Regelungs- und Betriebsschemata für elektrische Energieversorgungssysteme mit geringer Massenträgheit entwickelt wurde. Die wichtigsten Merkmale des Prüffelds sind seine Flexibilität zur schnellen Implementierung und Prüfung komplexer Regelungsalgorithmen, die von der Regelung einzelner Komponenten auf niedriger Ebene bis hin zu verteilten und systemweiten Regelungen reichen, seine Fähigkeit, mit verschiedenen Netztopologien konfiguriert zu werden, und die effiziente Emulation häufig beobachteter Parameterunsicherheiten und Störungen. Die detaillierte Beschreibung des PHiL-Prüffelds wird durch eine Leistungsdemonstration anhand einer Fallstudie ergänzt.

Schlagwörter: elektrische Energiesysteme mit geringer Trägheit; Intelligente Netze; power-hardware-in-the-loop-test; Verteilte Regelungsanwendungen.

***Corresponding author: Ismael Jaramillo-Cajica**, Chair of Control Systems and Network Control Technology, Brandenburg University of Technology, Cottbus-Senftenberg, Germany,
E-mail: jaramism@b-tu.de
Ajay Krishna, Chair of Control Systems and Network Control Technology, Brandenburg University of Technology, Cottbus-Senftenberg, Germany
Sabine Auer, Elena International GmbH, Berlin, Germany
Johannes Schiffer, Chair of Control Systems and Network Control Technology, Brandenburg University of Technology, Cottbus-Senftenberg, Germany; and Fraunhofer Research Institution for Energy Infrastructures and Geothermal Systems (IEG), 03046 Cottbus, Germany

1 Motivation

To reduce greenhouse gas emissions and fossil fuel consumption in the area of energy systems, the worldwide usage of renewable energies has increased remarkably in recent years [1]. Two key aspects of this transition are the integration of a larger number of geographically dispersed small-capacity distributed generation (DG) units based on renewable energy sources (RESs) that are interfaced to the grid through power-electronic inverters (often termed as *inverter-based* DGs) as well as the need for advanced control and communication technologies [2–4]. The physical differences between inverter-based DGs and conventional fossil fuel-driven rotating machines imply a reduction in the overall power system inertia, thus potentially decreasing the system robustness against disturbances [5, 6]. Such power systems with a high share of inverter-based DGs and loads are therefore commonly termed as *low-inertia power systems*.

The new structural and dynamical properties of low-inertia power systems result in the need for novel intelligent control and operation strategies suitably tailored to such systems. An important aspect thereby is that due to these substantial changes in the system properties, the mere usage of simulation-based studies for performance demonstration and validation of novel control and operational schemes has become insufficient. In other words, the need for testing facilities to accelerate the design and evaluation process has become crucial [7].

For such purposes, hardware-in-the-loop (HiL) test environments are a well-established concept for control system design and evaluation [8]. The HiL methodology facilitates the development and test of complex systems with different applications in the industry by combining a real-time simulation platform with hardware and/or control devices under test. The power-hardware-in-the-loop (PHiL) concept is an extension of the conventional HiL approach to power (systems) applications [9]. The main modification in PHiL compared to HiL is the inclusion of actual (electric) power in the loop, which results in a physical testbed for power system components, such as inverters, synchronous generators (SGs) or protection devices, their controls, and even interconnected power systems. Thus, the addition of power together with the flexibility provided by the HiL framework puts PHiL testbeds at a highly promising position for versatile testing and validation of low-inertia power systems applications, both at an equipment level and also at a system-wide level [10]. In addition to hardware-related testing, PHiL testbeds also facilitate advanced testing of cyber-physical features in low-inertia power systems. As a consequence, several PHiL testbed facilities have been successfully established in different countries during the last decade for education and research purposes [7, 11, 12]. A comprehensive survey on such testbeds is provided in [13].

Motivated by the aforementioned advantages and importance of PHiL systems, a PHiL testbed facility for low-inertia power systems (230/400 VAC, 750 VDC, 110 kW) has been developed at the Control Systems and Network Control Technology department at the Brandenburg University of Technology (BTU), Cottbus-Senftenberg, Germany. The following are the key attributes of the PHiL testbed at BTU:

1. Functionality to operate as an AC, a DC, or a hybrid (AC and DC) low-inertia power system.
2. Flexibility to emulate a large variety of system and network configurations.
3. Deployment of control, operation, and estimation algorithms for individual components as well as interconnected systems in a rapid-prototyping fashion with the aid of real-time control units, which can be programmed directly from Matlab/Simulink.
4. Emulation of commonly observed disturbances and parameter uncertainties in low-inertia power systems, such as heterogeneous dynamics, fluctuating power flows, and cyber-physical properties.

The remainder of the paper is organized as follows. At first, we explain the characteristics and technical information of the hardware components, and then a comprehensive description of the key testing and validation capabilities, with a special focus on using custom-made control algorithms is presented. Subsequently, the testbed capabilities are illustrated via experimental results of a practically relevant use case and finally, we summarize the conclusions.

2 Composition and structure of the testbed

In this section, we introduce the electrical characteristics and technical details of the components in the PHiL testbed. The system has a total installed power of 110 kW and can be operated either as a single- and three-phase AC system (230/400 VAC) or as a DC system (±350 VDC, 750 VDC). The current setting of the test facility allows to electrically interface a grid emulator (GE) unit (50 KW) and four DG units (15 kW each) via a power line emulator

Figure 1: A photograph of the PHiL testbed facility. From left to right: Grid emulator (GE) unit, power line emulation cabinet and four distributed generation (DG) units.

cabinet,[1] see Figure 1. The technical details of the GE unit and the DG units are summarized in Table 1[2] and their characteristics are detailed next.

2.1 GE unit

The GE unit (50 kW) is a programmable power amplifier able to convert its three-phase 230/400 VAC power input (BTU grid) into a variable AC or DC power output. The unit comprises a three-phase four-wire AC/DC-DC/AC bidirectional converter equipped with a real-time control unit and is capable of emulating the dynamics of large-scale grids, different types of electric loads, and network disturbances.

The electrical hardware in the GE unit consists of a bidirectional AC to DC active bridge rectifier (ABR) with an LCL input filter, a common split DC link in a back-to-back configuration, and a bidirectional DC to AC converter (CONV) with an LC(L) output filter, and a real-time control unit, see Figure 2a. Both the ABR and the CONV stages consist of three-phase two-level insulated gate bipolar transistor (IGBT) bridges whose output is regulated via pulse width modulation (PWM) signals.

The real-time control unit used in the GE is a powerful computer specifically designed for creating a model-based PHiL simulation platform as well as a communication infrastructure among the testbed components. This computer runs a Matlab/Simulink-compatible software, which allows generating time series and design control algorithms via standard Matlab/Simulink block models.

Table 1: Technical details of the GE and DG units.

General information		
	GE	**DG**
Rated power (kW/kVA)	50	15
Input voltage (VRMS)	400	400
Maximum DC link voltage (VDC)	860	800
IGBT switching frequency (kHz)	15	15
Output specifications		
AC voltage range (VRMS)	[25, 277]	[0, 400]
AC rated current (ARMS)	±65	±20
AC frequency range (Hz)	[10, 400]	[10, 400]
DC unipolar voltage range (VDC)	[20, 750]	[20,750]
DC bipolar voltage range (VDC)	[−350, 350]	[−350, 350]
DC rated current (A)	±47	±20

The control operation of the GE unit can be split into two layers. For the upper control layer, the real-time control unit processes the available voltage and current measurements at the PCC (see Figure 2a) and generates a set point signal w which is then transmitted to a digital signal processor (DSP) embedded in the power amplifier. Within this DSP, there are a set of predefined controllers for the ABR and the CONV stages that compute and generate the control signal u which is then provided to the IGBTs. Further details on the control architecture and how the set point w can be calculated are explained in the next section.

The real-time control unit can also exchange information with a main system control center for analysis, control, and performance monitoring purposes. In this regard, for synchronizing the timestamps of the measurements in different real-time control units, a precision time protocol (PTP) is employed [14]. This is necessary since – as in any real-world application – the clocks of the real-time control units are not synchronized [15]. Furthermore, direct peer-to-peer communication with other control units is also possible via a distributed communication network.

2.2 DG units

The DG units (15 kW each) can convert their 230/400 VAC three-phase input power (BTU grid supply) into a variable AC or DC output power for emulating the power generation/demand profiles and dynamics of various inverter-based RESs. These units have a similar composition in comparison to the GE unit, i.e., each DG unit consists of a three-phase four-wire AC/DC-DC/AC bidirectional converter equipped with its corresponding real-time control unit. However, differently from the GE, the DG units are specifically designed, such that both the high- (i.e., the outer) and the low-level (i.e., the inner-loop) control layers

1 An additional 20 kW SG will be interfaced with the current setup during the course of 2022.

2 A unipolar DC output consists of three positive voltage supplies (one on each phase). A bipolar DC output consists of a positive, a negative, and a reference voltage supply.

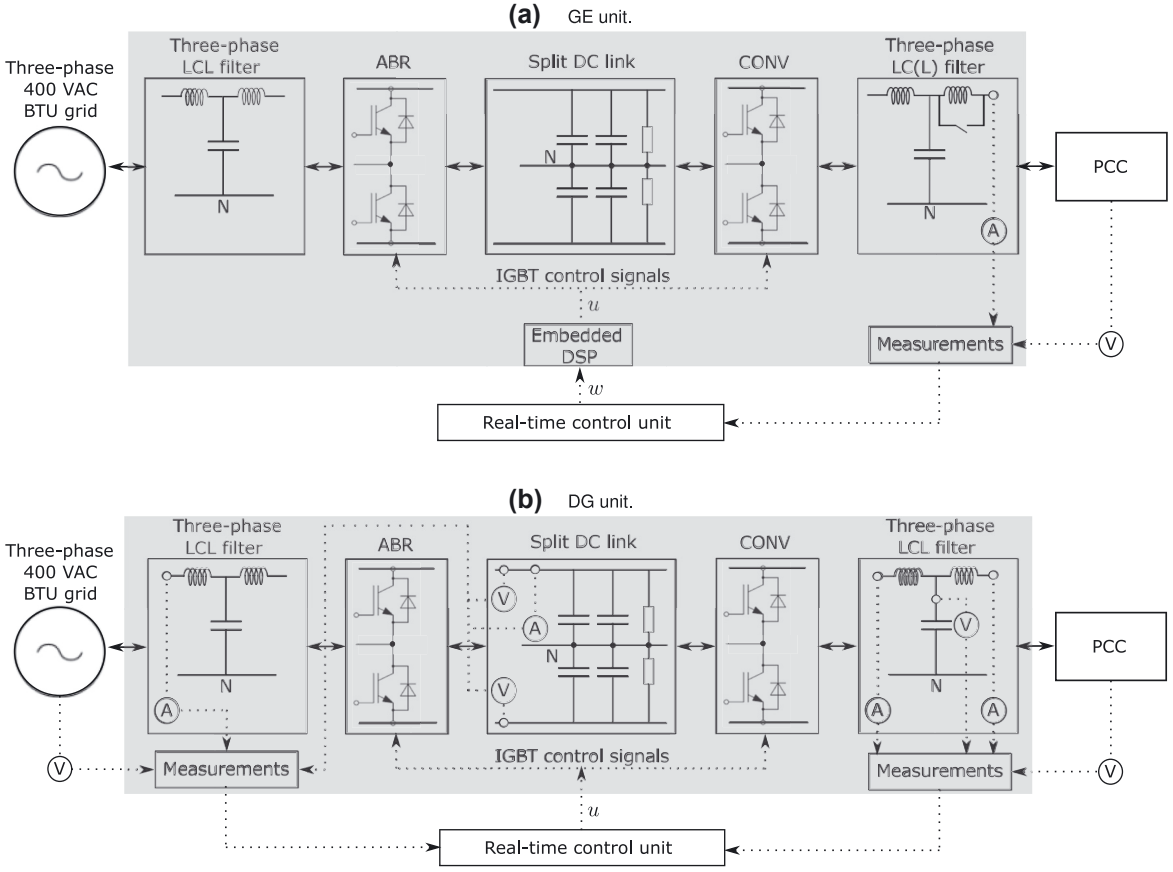

Figure 2: Schematic representation of single-phase equivalent circuits corresponding to the GE and the DG units. Bold lines represent electrical connections, while dotted lines represent signal connections. The control signals provided to the insulated gate bipolar transistors (IGBT) of the active bridge rectifier (ABR) and converter (CONV) stages are denoted by u. The converter output is interfaced with the low-inertia power system at the point of common coupling (PCC).

can be fully dictated by the corresponding real-time control unit.

For this reason, the DG unit possesses a larger number of measurement devices compared to the GE unit (see Figure 2b). The sensor information and the control inputs for the IGBTs are exchanged between the converter and real-time control unit through their input/output (I/O) modules. These features provide a flexible platform for designing and testing a wider spectrum of customized control algorithms, e.g., from decentralized and distributed hierarchical control strategies to customized inner-loop controllers for the ABR and the CONV. A detailed explanation of the control structures possible with the DG units is provided in the next section.

2.3 Power line emulation cabinet

This element allows us to electrically interconnect the GE and the DG units under different topologies as well as to simulate multiple types of short circuit events. The cabinet contains the π-equivalent circuits of two 0.5 km, two 10 km, and two 15 km distribution lines. The line parameter values are taken from real-world medium voltage 20 kV power lines and scaled to the laboratory setting with base values of 20 kV/20 MW for the original data and 400 V/100 kW for the laboratory, respectively. The structure of the cabinet allows connecting the power lines in a cascade manner for emulating additional power line circuits. In addition, it is possible to induce phase-to-neutral and phase-to-phase short circuits on any power line by closing the contactors $K1$ to $K6$ as shown in Figure 3.

A combination of the aforementioned components results in the current PHiL testbed, which is depicted in Figure 4.

3 Key testing and validation capabilities

Building upon the hardware architecture explained in Section 2, in this section, we showcase the main control,

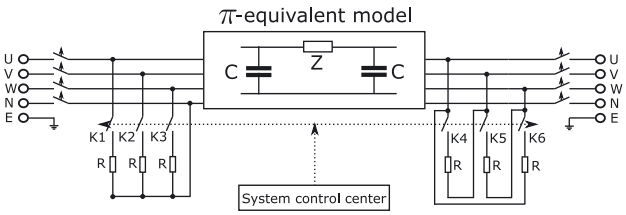

Figure 3: Schematic diagram of a threephase power line in the power line emulator cabinet, where a π-equivalent circuit and short circuit contactors are embedded.

testing, and validation capabilities of the PHiL testbed. We start with the functionalities and flexibility regarding the control implementation. Then, we explain how some of the important physical and cyber-physical disturbances observed in low-inertia power systems can be emulated in the laboratory.

3.1 Control functionality

Often, in grid-connected power converters, a cascaded control structure is employed [16–18]. In such cases, the inner-loop control takes care of the fundamental control tasks, such as tracking of a current or voltage reference, and disturbance rejection, e.g. harmonics. The outer-loop control is then responsible for grid-related control tasks, such as the provision of ancillary services.

In standard PHiL applications, power amplifiers are used as power sources [10]. Then, the inner-loop controls are readily provided by the manufacturer, which implies that they cannot be freely adjusted by the user. Yet, in the context of low-inertia systems, this may be unsatisfactory, since already the dynamics of the inner-loop controls may impact the system stability [5, 6]. Likewise, the dynamics of frequently employed phase-locked loop (PLL) algorithms become increasingly relevant [5, 19]. Furthermore, the design of novel control schemes for low-inertia systems may require a complete redesign of the converter control structure [20, 21].

These considerations are taken into account in the system design of the four DG units in the PHiL testbed, where the operator has direct access to the reference signal provided to the IGBTs (signal u in Figure 2b). More precisely, the designer has the full flexibility to implement inner-loop controllers, e.g. following standard approaches [17, 22], or any other sort of converter control, e.g., synchronverter algorithms [20], as well as observer and estimation algorithms, such as for PLLs [17, 23]. Any such implementation can be done directly from Matlab/Simulink. This results in an efficient and easily accessible workflow since many control engineers are familiar with the Matlab/Simulink environment. For instance, to operate a DG unit in grid-feeding mode [16, 18], one can design the inner-loop current and power (or in some cases current) controllers in the converter, or for grid-forming operation, one can implement the inner-loop voltage and current controllers [16, 18, 24]. An example for the latter is schematically

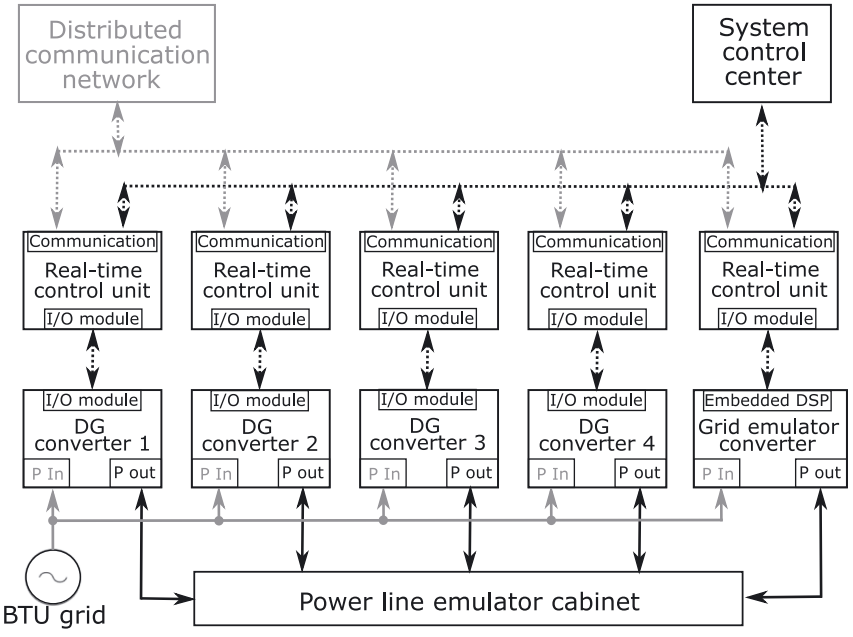

Figure 4: Schematic diagram of the overall PHiL testbed architecture. Solid lines represent electrical connections while dotted lines represent signal connections.

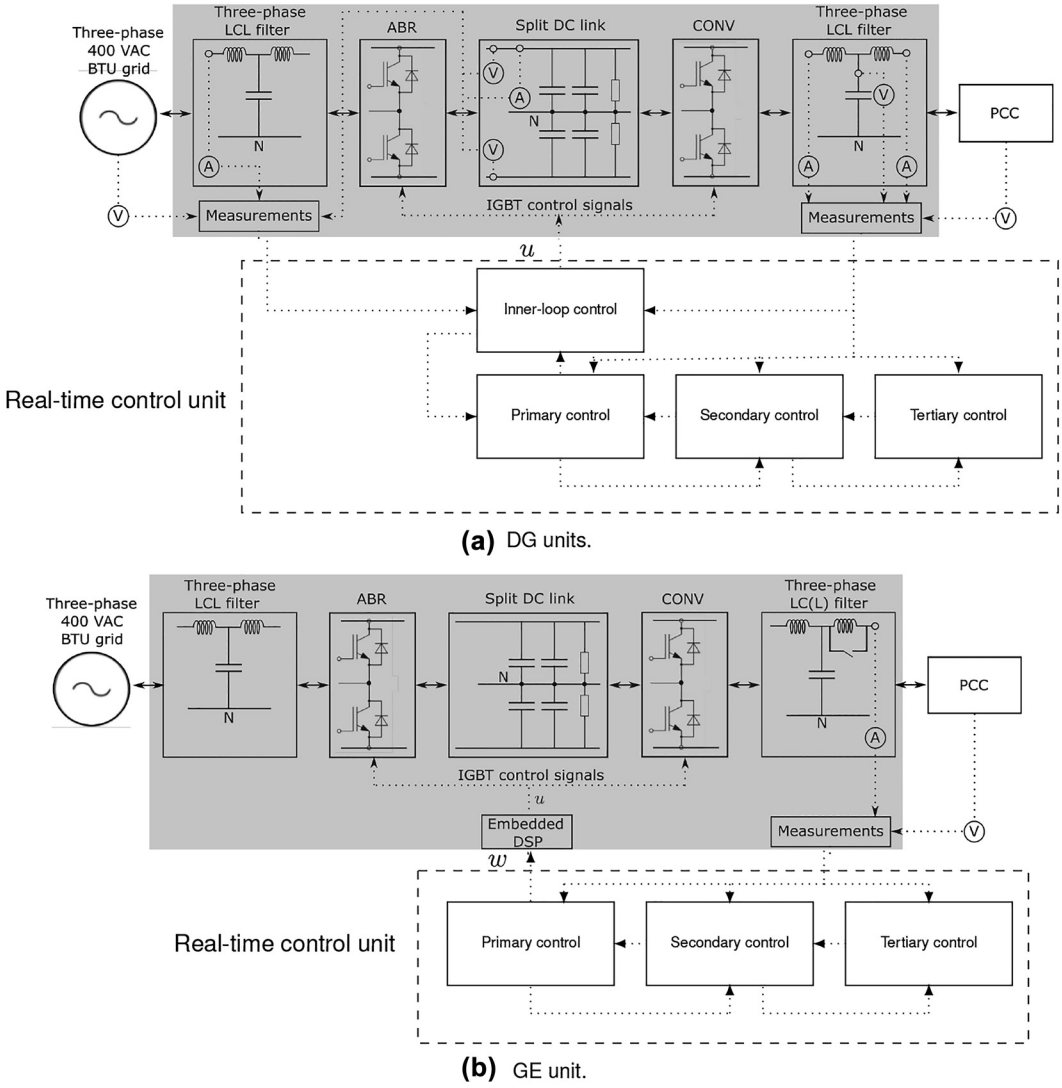

Figure 5: Exemplary hierarchical control architecture for the DG units and the GE unit in the PHiL testbed: (a) The control signal u provided to the IGBTs of the ABR and the CONV stages is generated by the real-time control unit, (b) the setpoint w provided to the embedded DSP is generated by the real-time control unit.

introduced in Figure 6.[3] The aforementioned functionality with the DG units is a highlighting feature of the PHiL testbed.

Recall from Section 2 that in comparison to the DG units, the GE unit is a standard power amplifier. That is, the inner-loop controls are already implemented (in the embedded DSP) and as an operator, we can specify the set points, i.e., the signal w in Figure 2a, either in terms of voltage or current. This is considered admissible, since the GE unit is intended to emulate the dynamics of a larger power system. In such a setting, a direct control of the IGBTs is not necessary, as the fast dynamics of the power electronics (including their inner-loop controls) are less relevant as in the case of individual DG units. Alternatively, the GE set points can also be calculated by using a higher-level controller, e.g., primary and secondary controllers.

The aforementioned control features for the DG units and the GE units are schematically explained in Figure 5.

3.2 Physical and cyber-physical disturbance generation

In low-inertia power systems, the multitude of disturbances and uncertainties is much higher than that of a conventional power system [3, 4]. The core reason for that is the wide variety of dynamical components present in

3 Signals with subscript *abc* and *dq* denote three-phase *abc* signals and *dq* signals, respectively.

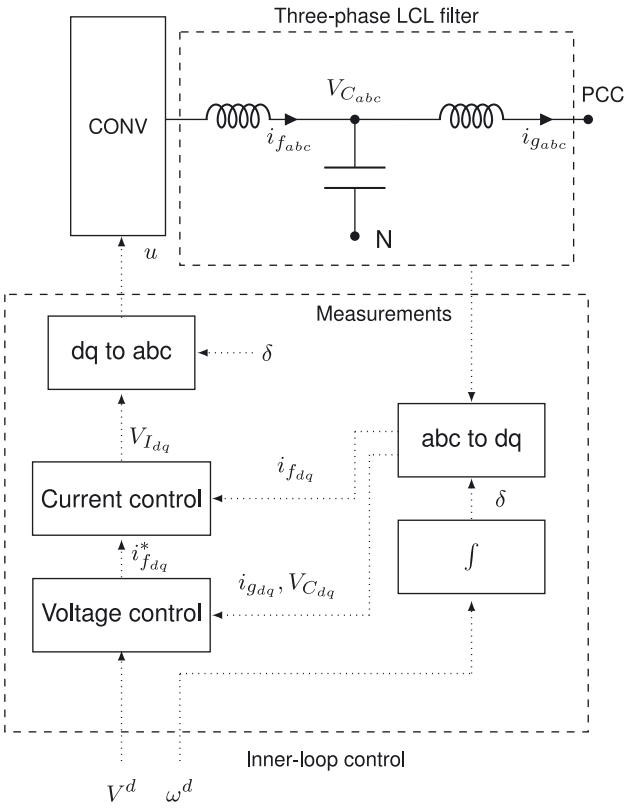

Figure 6: Schematic representation of a DG unit operating in grid-forming mode [16, 18, 24]. The CONV stage is connected to the PCC via a three-phase LCL filter, see also Figure 2b. In grid-forming mode, the voltage at the capacitor is regulated by using a cascaded current and voltage control (e.g., a proportional integral (PI) control in *dq* coordinates). The control signal u is then provided directly to the IGBTs of the CONV stage.

such networks, which mainly stems from the difference in dynamics between inverter-based RESs and the uncertainties introduced by renewable energy generation. On top of that, the addition and/or removal of RESs and loads also add up to the overall disturbances in the network. Thus, for testing and validating low-inertia power systems in a realistic environment, the need for emulating the aforesaid disturbances and uncertainties is crucial.

In the PHiL testbed, we have a flexible feature with which one–with the access to the references provided directly to the PWM signals of the DG units (recall Figure 5a)–can design any dynamical behavior of an inverter-interfaced RES, e.g., grid-forming inverters, grid-feeding inverters and photovoltaic or wind parks.

In contrast to the physical dynamical disturbances and uncertainties, a wide variation of cyber-physical control-related disturbances can be realized by using the real-time control units, such as communication delays [25], clock drifts [15] or denial-of-service attacks [26, 27].

As an example, if we want to emulate a communication delay, one could use the standard delay blocks in Matlab/Simulink together with the communication interface provided by the real-time control units. Furthermore, for studying the phenomenon of clock drifts [28], we utilize the advantage of having five real-time control units (instead of just one central unit) to facilitate distributed digital computation (the main reason for clock drifts) [15].

4 Experimental case study

In this section, we present a detailed description of an experimental case study that demonstrates several of the main features of the PHiL testbed facility. The experimental setup emulates the behavior of a low-inertia power network with topology shown in Figure 7. In this setting, the GE emulates a larger power system, DG 1 operates as grid-supporting unit [16] and DG 2 operates as a constant power load. The motivation to choose such a configuration for the experimental case study is two-fold. On one hand we want to demonstrate that higher-level control laws can be implemented at the GE unit (see Figure 5b), e.g., a larger power network represented by the second order swing equation representing the aggregated frequency dynamics of all SGs in the power system [29, 30]. On the other hand, we want to show that one can design the inner-loop controllers of the DG units (see Figure 5a) for emulating grid-supporting and constant power load dynamics.

Following [29, 30], the frequency dynamics of a larger power system are emulated by the GE unit via the aggregated swing equation

$$\begin{aligned} \dot{\delta} &= \omega, \\ M\dot{\omega} &= -D(\omega - \omega^d) + P_m - P_e, \end{aligned} \tag{4.1}$$

where $\delta : \mathbb{R}_{\geq 0} \to \mathbb{R}$ is the phase angle, $\omega : \mathbb{R}_{\geq 0} \to \mathbb{R}_{>0}$ is the rotational speed, $M \in \mathbb{R}_{>0}$ is the moment of inertia of the aggregated rotor masses of the generators in the power

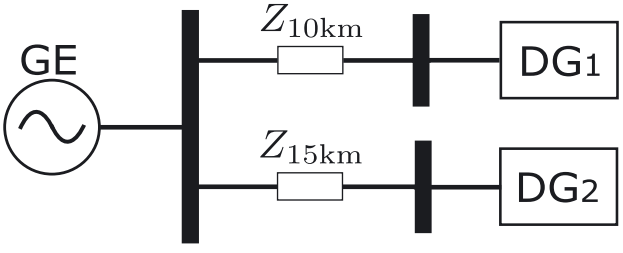

Figure 7: Electrical topology of the experimental case study. The impedances $Z_{10\text{ km}}$ and $Z_{15\text{ km}}$ represent the π-equivalent power line circuits shown in Figure 4.

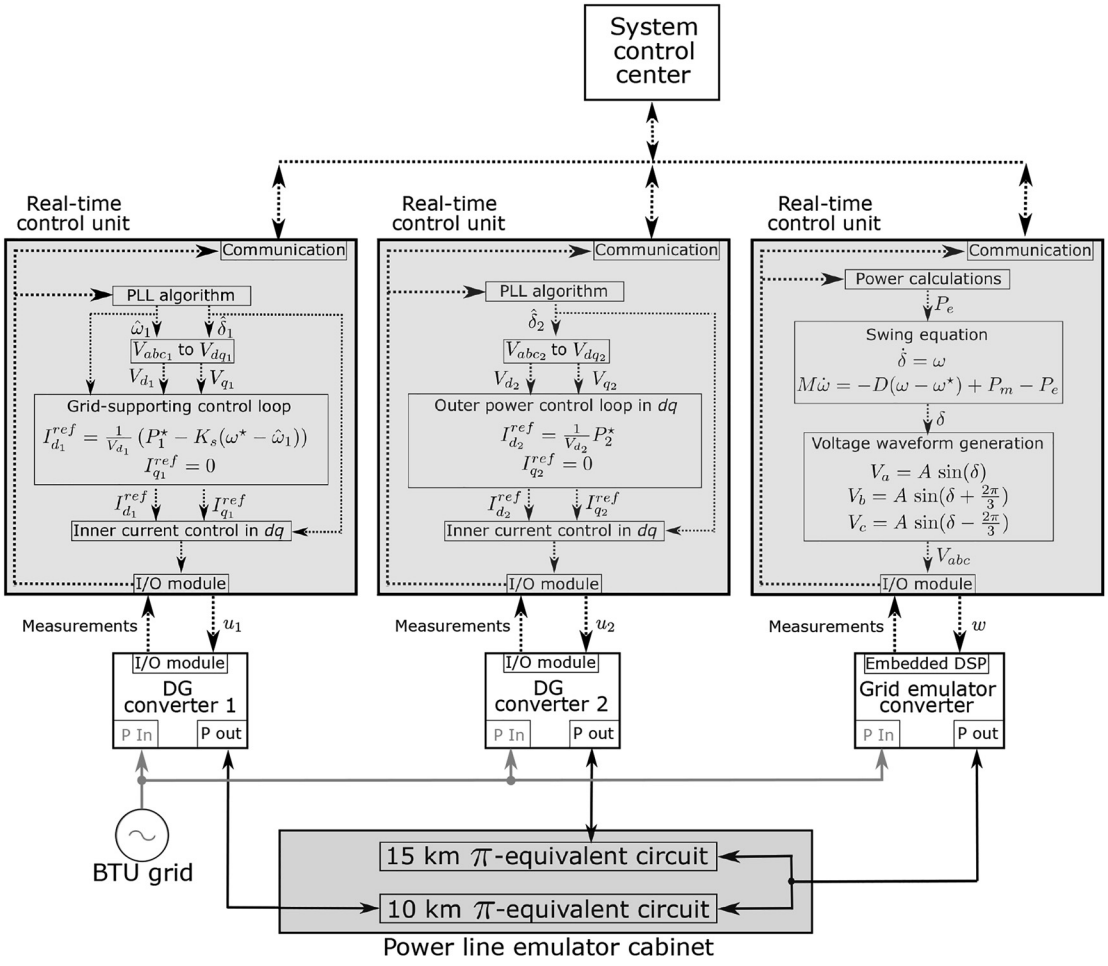

Figure 8: A schematic of the experimental configuration, where the GE unit is connected to two DG units via 15 km and 10 km power lines, see Figure 7. The GE unit emulates the frequency dynamics of a larger power system via the second order swing Equation (4.1) the DG unit 1 operates as a grid-supporting unit [16] and DG unit 2 operates as a constant power load.

system, $\omega^d \in \mathbb{R}_{>0}$ is the desired synchronous speed, and $D \in \mathbb{R}_{>0}$ is a damping factor. Furthermore, $P_m : \mathbb{R}_{\geq 0} \to \mathbb{R}_{>0}$ and $P_e : \mathbb{R}_{\geq 0} \to \mathbb{R}_{>0}$ are the mechanical power input and the electrical power output, respectively.

As mentioned previously, DG unit 1 is operated as a grid-supporting unit, whose main objectives are to feed/consume a specific amount of power[4] and the same time, support in keeping the network frequency close to the nominal value [16]. The latter objective is realized with the use of a proportional control law [16]. For the aforementioned setting, the real-time control unit in the DG unit 1 regulates the output of the ABR stage through a standard proportional resonant (PR) controller [22], while, for realizing grid-supporting mode, the output power of the CONV stage is controlled by a PI controller in *dq*-coordinates [16, 22]. Finally, the control of DG unit 2 is also implemented in a similar way as that of DG unit 1, where the main difference is that DG unit 2 is operated as a constant power load. The experimental configuration mentioned so far is schematically detailed in Figure 8.

At first, we operate DG unit 1 without the grid-supporting capability, i.e., the frequency regulation term depicted in the real-time control unit box of DG unit 1 in Figure 8 is inactive ($K_s = 0$). Then, DG unit 1 operates as a constant power source/load (depending on the power setpoint $P_1^\star$ provided to it). For simplicity, throughout the experiment, we set $P_1^\star = 0$ W. At around 5 s, we change the power setpoint of DG unit 2 ($P_2^\star$ in Figure 8) to -5 kW, i.e., DG unit 2 is operating as a constant power load that consumes 5 kW. The experimental result with this setting is depicted in Figure 9a, where a frequency drop from 50 Hz to 48.95 Hz can be seen. The change in frequency

4 In grid-supporting mode, the setpoints can also be specified in terms of current [16].

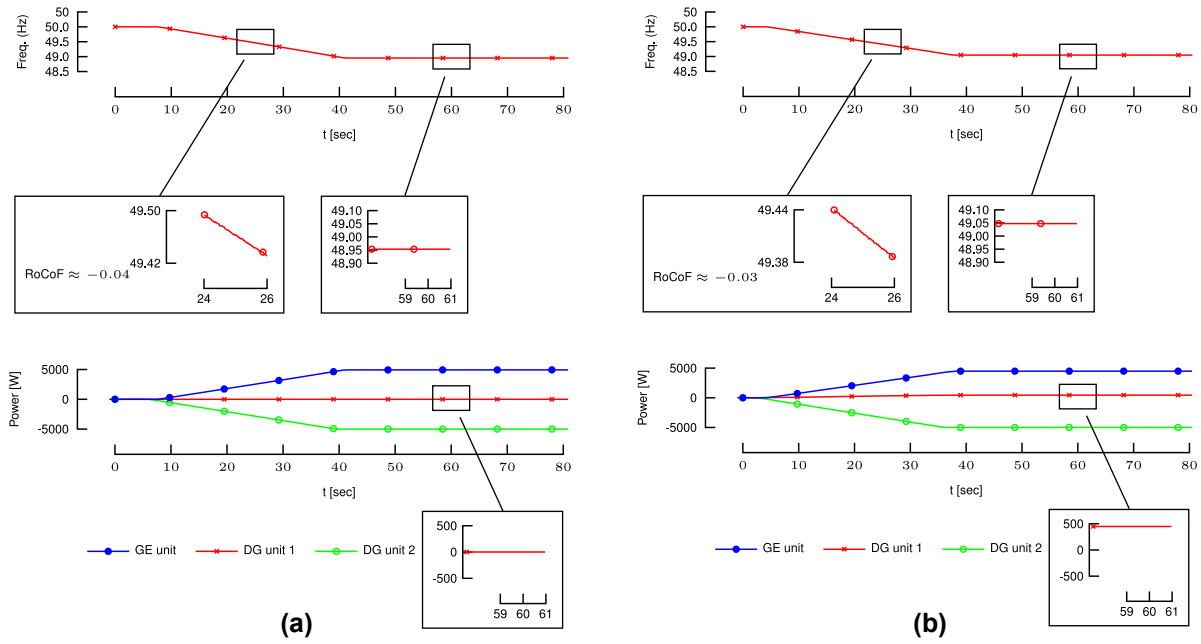

Figure 9: Frequency and active power plots for the experimental scenario. At around 5 s, the active power setpoint of the distributed generation (DG) unit 2 $(P_2^\star)$ is changed to −5 kW. (a) Case 1: Grid-supporting action in DG unit 1 is inactive. Observe that the frequency drops to 48.95 Hz, see the zoomed frequency plot at 60 s. Furthermore, the rate of change of frequency (RoCoF) is approximately −0.04 and note that DG unit 1 does not inject/consume any active power, see the zoomed power plot at 60 s, (b) Case 2: Grid supporting action in DG unit 1 is active. Observe that the frequency drops only to 49.05 Hz, see the zoomed frequency plot at 60 s. Furthermore, the RoCoF is approximately −0.03 and note that DG unit 1 also injects an active power of approximately 500 W, see the zoomed power plot at 60 s.

in correspondence to a change in active power in the network is due to the swing equation dynamics (see (4.1)) implemented at the GE unit.

In the second phase of the experiment, we activate the grid-supporting action of DG unit 1 by choosing a positive value for the control gain K_s (see the real-time control unit block of DG unit 1 in Figure 8). We fix the active power setpoints of DG units 1 and 2 to the same value as before, i.e., $P_1^\star = 0$ W and $P_2^\star = -5$ kW. The experimental result for this scenario is shown in Figure 9b, where it can be seen that the frequency drop has decreased i.e., from 48.95 Hz (without grid-supporting action, see Figure 9a) to 49.05 Hz (with grid-supporting action). Similarly, a drop in the rate of change of frequency (RoCoF) can also be observed from the mode without grid-supporting action (Figure 9a) to the mode with grid-supporting action (Figure 9b), i.e., from RoCoF ≈ -0.04 to RoCoF ≈ -0.03. In principle, by choosing a higher value for the gain K_s in the grid-supporting controller (recall Figure 8), the frequency drop from the nominal value (50 Hz) and the RoCoF can be further reduced. However, choosing a wider range of values for the gain K_s and studying the steady-state and transient properties of the frequency trajectory is beyond the scope of this paper and the reader is referred to [16] for more details.

5 Conclusions

Due to the increasing challenges encountered in designing and operating low-inertia power systems, the need for flexible testing facilities is inevitable. In this paper, we have presented a PHiL testbed facility that serves as a platform for testing and validating AC and DC low-inertia power networks with different topologies, cyber-physical characteristics, and custom-made controllers among other settings. Experimental results showed that the presented testbed is suitable for studying realistic and practically relevant case studies in a flexible and versatile fashion.

As a next step, we will incorporate an SG (and its corresponding real-time control unit) into the current setting such that a wider spectrum of operation scenarios in low-inertia power systems can be emulated.

Author contributions: All the authors have accepted responsibility for the entire content of this submitted manuscript and approved submission.
Research funding: This work is partially supported by the Deutsche Forschungsgemeinschaft (DFG) project

CoCoMuSy - Project number 360332943 and the Bundesministerium für Wirtschaft und Klima (BMWK) project MARiE - Project number 03EI4012A-B.

Conflict of interest statement: The authors declare no conflicts of interest regarding this article.

References

[1] T. Klaus, C. Vollmer, K. Werner, H. Lehmann, and K. Müschen, "UBA. Energy target 2050: 100% renewable electricity supply," *Energieziel 2050*, pp. 8–13, 2010.

[2] R. Lasseter, "Microgrids," in *IEEE Power Engineering Society Winter Meeting, 2002*, vol. 1, IEEE, 2002, pp. 305–308.

[3] N. Hatziargyriou, H. Asano, R. Iravani, and C. Marnay, "Microgrids," *IEEE Power Energy Mag.*, vol. 5, no. 4, pp. 78–94, 2007.

[4] A. Hirsch, Y. Parag, and J. Guerrero, "Microgrids: a review of technologies, key drivers, and outstanding issues," *Renewable Sustainable Energy Rev.*, vol. 90, pp. 402–411, 2018.

[5] F. Milano, F. Dörfler, G. Hug, D. J. Hill, and G. Verbič, "Foundations and challenges of low-inertia systems," in *2018 Power Systems Computation Conference (PSCC)*, IEEE, 2018, pp. 1–25.

[6] U. Markovic, O. Stanojev, P. Aristidou, E. Vrettos, D. Callaway, and G. Hug, "Understanding small-signal stability of low-inertia systems," *IEEE Trans. Power Syst.*, vol. 36, no. 5, pp. 3997–4017, 2021.

[7] G. Turner, J. P. Kelley, C. L. Storm, D. A. Wetz, and W. J. Lee, "Design and active control of a microgrid testbed," *IEEE Trans. Smart Grid*, vol. 6, no. 1, pp. 73–81, 2015.

[8] M. Bacic, "On hardware-in-the-loop simulation," in *Proceedings of the 44th IEEE Conference on Decision and Control*, IEEE, 2005, pp. 3194–3198.

[9] G. F. Lauss, M. O. Faruque, K. Schoder, C. Dufour, A. Viehweider, and J. Langston, "Characteristics and design of power hardware-in-the-loop simulations for electrical power systems," *IEEE Trans. Ind. Electron.*, vol. 63, no. 1, pp. 406–417, 2015.

[10] C. S. Edrington, M. Steurer, J. Langston, T. El-Mezyani, and K. Schoder, "Role of power hardware in the loop in modeling and simulation for experimentation in power and energy systems," *Proc. IEEE*, vol. 103, no. 12, pp. 2401–2409, 2015.

[11] C. Wang, X. Yang, Z. Wu, et al., "A highly integrated and reconfigurable microgrid testbed with hybrid distributed energy sources," *IEEE Trans. Smart Grid*, vol. 7, no. 1, pp. 451–459, 2016.

[12] V. Salehi, A. Mohamed, A. Mazloomzadeh, and O. A. Mohammed, "Laboratory-based smart power system, part I: design and system development," *IEEE Trans. Smart Grid*, vol. 3, no. 3, pp. 1394–1404, 2012.

[13] M. Cintuglu, O. Mohamme, K. Akkaya, and A. Uluagac, "A survey on smart grid cyber-physical system testbeds," *IEEE Commun. Surv. Tutor.*, vol. 19, no. 1, pp. 446–464, 2017.

[14] J. Eidson, M. Fischer, and J. White, "IEEE-1588 standard for a precision clock synchronization protocol for networked measurement and control systems," *IEEE*, vol. 1, pp. 1588–2019, 2019.

[15] A. Krishna, J. Schiffer, and J. Raisch, "Distributed secondary frequency control in microgrids: robustness and steady-state performance in the presence of clock drifts," *Eur. J. Control*, vol. 51, pp. 135–145, 2019.

[16] J. Rocabert, A. Luna, F. Blaabjerg, and P. Rodriguez, "Control of power converters in AC microgrids," *IEEE Trans. Power Electron.*, vol. 27, no. 11, pp. 4734–4749, 2012.

[17] R. Teodorescu, M. Liserre, and P. Rodriguez, *Grid Converters for Photovoltaic and Wind Power Systems*, vol. 29, UK, John Wiley & Sons, 2011.

[18] J. Schiffer, D. Zonetti, R. Ortega, A. Stanković, J. Raisch, and T. Sezi, "Modeling of microgrids – from fundamental physics to phasors and voltage sources," *Automatica*, vol. 74, no. 12, pp. 135–150, 2016.

[19] J. G. Rueda-Escobedo, S. Tang, and J. Schiffer, "A performance comparison of PLL implementations in low-inertia power systems using an observer-based framework," *IFAC-PapersOnLine*, vol. 53, no. 2, pp. 12244–12250, 2020.

[20] Q. C. Zhong and G. Weiss, "Synchronverters: inverters that mimic synchronous generators," *IEEE Trans. Ind. Electron.*, vol. 58, no. 4, pp. 1259–1267, 2010.

[21] C. Arghir, T. Jouini, and F. Dörfler, "Grid-forming control for power converters based on matching of synchronous machines," *Automatica*, vol. 95, pp. 273–282, 2018.

[22] F. Blaabjerg, *Control of Power Electronic Converters and Systems*, vol. 2, US, Elsevier Academic Press, 2018.

[23] J. G. Rueda-Escobedo, J. A. Moreno, and J. Schiffer, "Finite-time estimation of time-varying frequency signals in low-inertia power systems," in *2019 18th European Control Conference (ECC)*, IEEE, 2019, pp. 2108–2114.

[24] N. Pogaku, M. Prodanovic, and T. Green, "Modeling, analysis and testing of autonomous operation of an inverter-based microgrid," *IEEE Trans. Power Electron.*, vol. 22, no. 2, pp. 613–625, 2007.

[25] S. Alghamdi, J. Schiffer, and E. Fridman, "Synthesizing sparse and delay-robust distributed secondary frequency controllers for microgrids," *IEEE Trans. Control Syst. Technol.*, vol. 29, no. 2, pp. 691–703, 2019.

[26] C. Persis and P. Tesi, "Resilient control under denial-of-service," *IFAC Proc.*, vol. 47, no. 3, pp. 134–139, 2014.

[27] P. Srikantha and D. Kundur, "Denial of service attacks and mitigation for stability in cyber-enabled power grid," in *Power and Energy Society Innovative Smart Grid Technologies Conference (ISGT)*, 2015.

[28] N. M. Freris, S. R. Graham, and P. R. Kumar, "Fundamental limits on synchronizing clocks over networks," *IEEE Trans. Autom. Control*, vol. 56, no. 6, 2011. https://doi.org/10.1109/tac.2010.2089210.

[29] T. Weckesser and T. Van Cutsem, "Equivalent to represent inertial and primary frequency control effects of an external system," *IET Gener. Transm. Distrib.*, vol. 11, no. 14, pp. 3467–3474, 2017.

[30] J. Schiffer, P. Aristidou, and R. Ortega, "Online estimation of power system inertia using dynamic regressor extension and mixing," *IEEE Trans. Power Syst.*, vol. 34, no. 6, pp. 4993–5001, 2019.

Bionotes

Dr. Ajay Krishna
Chair of Control Systems and Network Control Technology, Brandenburg University of Technology, Cottbus-Senftenberg, Germany
Ajay.Krishna@b-tu.de

Dr. Ajay Krishna is a research associate working at the Chair of Control Systems and Network Control Technology, Brandenburg Technical University, Cottbus, Germany. His research interests are in the area of modeling and control of power networks with a high share of renewables.

MSc. Ismael Jaramillo-Cajica
Chair of Control Systems and Network Control Technology, Brandenburg University of Technology, Cottbus-Senftenberg, Germany
jaramism@b-tu.de

MSc. Ismael Jaramillo-Cajica is currently pursuing a Ph.D. degree with the Department of Control Systems and Network Control Technology at the Brandenburg University of Technology Cottbus-Senftenberg (BTU). His current research interests include control of converter-based distributed generators and analysis of interconnected low-inertia power systems.

Dr. Sabine Auer
Elena International GmbH, Berlin, Germany
sabine.auer@elena-international.com

Dr. Sabine Auer holds a PhD in physics from the Potsdam Institute for Climate Impact Research and has more than ten years of experience in the field of renewable energy and energy systems analysis. She is working in the fields energy system optimization and power grid stability analyses. As such she is contributing to the Open-Source development of software (namingly PowerDynamics.jl) for the transient stability analysis of inverter-based power grids.

Prof. Dr.-Ing. Johannes Schiffer
Chair of Control Systems and Network Control Technology, Brandenburg University of Technology, Cottbus-Senftenberg, GermanyFraunhofer Research Institution for Energy Infrastructures and Geothermal Systems (IEG), 03046 Cottbus, Germany
schiffer@b-tu.de

Prof. Dr.-Ing. Johannes Schiffer received the Diploma degree in engineering cybernetics from the University of Stuttgart, Germany, in 2009 and the Ph.D. degree (Dr.-Ing.) in electrical engineering from Technische Universität (TU) Berlin, Germany, in 2015. He currently holds the chair of Control Systems and Network Control Technology at Brandenburgische Technische Universität Cottbus-Senftenberg, Germany and leads the business area Control, Automation and Operation Managemement at the Fraunhofer Research Institution for Energy Infrastructures and Geothermal Systems (IEG). Prior to that, he has held appointments as Lecturer (Assistant Professor) at the School of Electronic and Electrical Engineering, University of Leeds, U.K. and as Research Associate in the Control Systems Group and at the Chair of Sustainable Electric Networks and Sources of Energy both at TU Berlin. In 2017 he and his co-workers received the Automatica Paper Prize over the years 2014-2016. His current research interests include distributed control and analysis of complex networks with application to microgrids and smart energy systems.